REPORT DOCUMENTATION PAGE

Form Approved OMB No. 0704-0188

1. REPORT DATE *(DD-MM-YYYY)*	2. REPORT TYPE	3. DATES COVERED *(From - To)*
	Technical Papers	

4. TITLE AND SUBTITLE

5a. CONTRACT NUMBER

5b. GRANT NUMBER

5c. PROGRAM ELEMENT NUMBER

6. AUTHOR(S)

5d. PROJECT NUMBER
2303

5e. TASK NUMBER
M2C8

5f. WORK UNIT NUMBER

7. PERFORMING ORGANIZATION NAME(S) AND ADDRESS(ES)

Air Force Research Laboratory (AFMC)
AFRL/PRS
5 Pollux Drive
Edwards AFB CA 93524-7048

8. PERFORMING ORGANIZATION REPORT

9. SPONSORING / MONITORING AGENCY NAME(S) AND ADDRESS(ES)

Air Force Research Laboratory (AFMC)
AFRL/PRS
5 Pollux Drive
Edwards AFB CA 93524-7048

10. SPONSOR/MONITOR'S ACRONYM(S)

11. SPONSOR/MONITOR'S NUMBER(S)

12. DISTRIBUTION / AVAILABILITY STATEMENT

Approved for public release; distribution unlimited.

13. SUPPLEMENTARY NOTES

14. ABSTRACT

1121 005

15. SUBJECT TERMS

16. SECURITY CLASSIFICATION OF:			17. LIMITATION OF ABSTRACT	18. NUMBER OF PAGES	19a. NAME OF RESPONSIBLE PERSON
a. REPORT	b. ABSTRACT	c. THIS PAGE			Leilani Richardson
Unclassified	Unclassified	Unclassified	A		19b. TELEPHONE NUMBER *(include area code)* (661) 275-5015

62 Separate items are enclosed.

2303M1C8 TP-FY99-0049
F0461-93-C-0005
✓ Spreadsheet
✓ DTS

MEMORANDUM FOR PRR (Contractor Publication)

FROM: PROI (TI) (STINFO)

4 March 1999

SUBJECT: Authorization for Release of Technical Information, Control Number: AFRL-PR-ED-TP-FY99-0049
Jerry Boatz et al., "Experimental and Theoretical Characterization of the Oxygen-coordinated Donor-Adducts of $COCl_2$, COClF and COF_2 with AsF_5 and SbF_5"

Journal article

(Public Release)

Experimental and Theoretical Characterization of the Oxygen-coordinated Donor-Acceptor Adducts of $COCl_2$, COClF and COF_2 with AsF_5 and SbF_5

Berthold Hoge,[†§] Jerry A. Boatz[‡] and Karl O. Christe[†,‡,*]

Loker Hydrocarbon Research Institute, University of Southern California, Los Angeles, California 90089-1661, and Air Force Research Laboratory, Edwards Air Force Base, California 93524

Abstract

When reacted with an excess of the corresponding carbonyl halides, AsF_5 and SbF_5 from the following 1:1 adducts: $COCl_2 \bullet AsF_5$, $COCl_2 \bullet SbF_5$, $COClF \bullet AsF_5$, $COClF \bullet SbF_5$, $COF_2 \bullet AsF_5$ and $COF_2 \bullet SbF_5$. All adducts are unstable at ambient temperature, and their dissociation enthalpies were determined from the dissociation pressure curves. Vibrational and multinuclear NMR spectra and theoretical calculations show that all compounds are oxygen-coordinated donor-acceptor adducts, and that the strengths of the oxygen-bridges increase from COF_2 to $COCl_2$ and from AsF_5 to SbF_5.

Introduction

In the course of an investigation of halocarbonyl cations,[1] it became necessary to study the competing Lewis base-Lewis acid interactions of the dihalocarbonyl compounds, $COCl_2$, COClF and COF_2, with AsF_5 and SbF_5. Although the individual dihalocarbonyl and Lewis acid molecules are well characterized, little is known about their interactions.[2]

For $COCl_2$, no reports on the $AsF_5/COCl_2$ system were found, and the only report on the $SbF_5/COCl_2$ system consists of a brief comment[3] that with a fivefold excess of SbF_5 in SO_2ClF solution at -78 °C a new signal was observed in the ^{13}C NMR spectrum, which was correctly attributed to the $COCl^+$ cation.[1] Other Lewis acids, which were studied in connection with $COCl_2$, include BF_3, BCl_3, $AlCl_3$, $AlBr_3$, $GaCl_3$, $SnCl_4$, $SbCl_5$, $MoCl_6$, WCl_6, and $PtCl_4$,[2] but only for

$AlCl_3$ [4,5] and possibly $SbCl_5$ [4,6] evidence was presented for the existence of oxygen-coordinated 1:1 donor-acceptor adducts.

For COClF, the only reports on an interaction with Lewis acids are two NMR studies[3,7] with SbF_5 in SO_2ClF solution. The results from these studies indicate the presence of an oxygen-coordinated donor-acceptor adduct at low temperatures and halogen exchange at higher temperatures.

For COF_2, the presence of thermally unstable, oxygen-coordinated donor-acceptor complexes with SbF_5 and AsF_5 were first demonstrated by low-temperature ^{19}F NMR measurements,[7] and subsequently confirmed by low-temperature Raman spectroscopy.[8] However, no physical properties were reported for these adducts, and no reports could be found on other COF_2•Lewis acid adducts.

Experimental Section

Materials and Methods. Carbonyl chloride (Matheson), COF_2 (PCR Research Chemicals), and AsF_5 (Ozark Mahoning) were used as received. Antimony pentafluoride (Ozark Mahoning) was distilled prior to use. The COClF was prepared by a literature method.[11]

The volatile materials were handled in a stainless steel vacuum line equipped with Teflon-FEP U-traps, 316 stainless steel bellows seal valves, and a Heise pressure gauge.[9] Nonvolatile materials were handled in the dry nitrogen atmophere of a glove box. Raman spectra were recorded on a Cary model 83 GT using 1.5 w of the 488 nm exciting line of an Ar ion laser and flame sealed Pyrex tubes as sample containers. A previously described[10] device was used for the recording of the low-temperature spectra. Infrared spectra were recorded on a Midac model M FTIR spectrometer. NMR spectra were measured on a Varian Model Unity 300 MHz NMR spectrometer equipped with a 5 mm variable-temperature broad band probe. Sealed capillaries, which were filled with acetone-d_6 as lock substance, TMS as ^{13}C reference and $CFCl_3$ or $C_6H_5CF_3$ as ^{19}F reference, were placed inside the NMR tubes.

For the dissociation pressure measurements, the 1:1 adducts of AsF_5 and SbF_5 with the carbonyl halides were preformed in a Teflon-FEP ampule, which was directly connected to a Heise pressure gauge. The equilibrium dissociation pressures were established for each temperature, approaching the equilibria from both sides, i.e., higher pressures and lower pressures. The thermochemical properties were derived in the same manner as previously described.[12] The method used for the tensiometric titration (vapor pressure-composition isotherm) of the AsF_5-COF_2 system has previously been described.[4]

Preparation of $COF_2 \cdot AsF_5$. Arsenic pentafluoride (3.75 mmol) and COF_2 (40.0 mmol) were combined in a ½" o.d. Teflon-FEP ampule at -196 °C. The mixture was stirred at -78 °C for 1 h with a magnetic stirring bar, resulting in a suspension of a white solid in liquid COF_2. The excess of COF_2 was pumped off at -126 °C, leaving behind the white, solid $COF_2 \cdot AsF_5$ adduct in quantitative yield. The adduct melts in the range of -45 to -42 °C. Dissociation pressure (temperature [°C], pressure [mm]): (-100, 2), (-95, 4), (-90, 7), (-85, 13), (-81, 20), (-75, 38), (-71, 58), (-70, 66), (-66, 98), (-65, 108), (-64, 119), (-63, 131), (-62, 140), (-60, 168), (-57, 211), (-55, 253). NMR (SO_2ClF, -60 °C): $COF_2 \cdot AsF_5$: $\delta(^{13}C)$ 137.8 ppm; $^1J(CF)$ 330 Hz; $\delta(^{19}F)$-16 ppm. COF_2: $\delta(^{13}C)$ 130.0 ppm; $^1J(CF)$ 313 Hz; $\delta(^{19}F)$-23 ppm.

Preparation of $COF_2 \cdot SbF_5$. A mixture of SbF_5 (16.8 mmol) and COF_2 (40.0 mmol) was reacted and the resulting white, solid 1:1 adduct isolated as described for $COF_2 \cdot AsF_5$. The yield of $COF_2 \cdot SbF_5$ was quantitative.

Preparation of $COClF \cdot AsF_5$. A mixture of AsF_5 (1.7 mmol) and COClF (30.2 mmol) was stirred at -78 °C for 1 h. The excess of COClF was pumped off at -110 °C, leaving behind $COClF \cdot AsF_5$ (1.7 mmol) as a white, solid powder melting in the range -42 to -39 °C. Dissociation

pressure (temperature [°C], pressure [mm]): (-87, 3), (-84, 4), (-82, 5), (-80, 6), (-79, 7), (-78, 8), (-77, 9), (-76, 10), (-75, 11), (-74, 14), (-73, 16), (-72, 18), (-71, 20), (-70, 22), (-69, 25), (-68, 28), (-67, 32), (-66, 35), (-65, 39), (-64, 44), (-63, 50), (-62, 56), (-61, 62), (-60, 68), (-59, 76), (-58, 85), (-57, 94), (-56, 104), (-55, 117), (-54, 128), (-53, 140), (-52, 157), (-51, 170), (-50, 192), (-49, 224), (-48, 247), (-47, 275), (-46, 298), (-45, 320), (-44, 342), (-43, 363), (-42, 380).

Preparation of $COClF \cdot SbF_5$. A mixture of SbF_5 (2.3 mmol) and COClF (15.6 mmol) was reacted as described for $COClF \cdot AsF_5$, resulting in the quantitative formation of the white, solid $COClF \cdot SbF_5$ adduct. NMR (SO_2ClF, -60 °C): $COClF \cdot SbF_5$: $\delta(^{13}C)$ 163.8 ppm; $^1J(CF)$383 Hz; $\delta(^{19}F)$ 73.9 ppm. COFCl: $\delta(^{13}C)$ 142.0 ppm; $^1J(CF)$ 368 Hz; $\delta(^{19}F)$ 59.7 ppm. Dissociation pressure (temperature [°C] pressure [mm]): (-43, 3), (-40, 9), (-38, 11), (-36, 14), (-34, 19), (-29, 35), (-25, 54), (-23, 70), (-20, 96), (-16, 139), (-15, 152), (-13, 173), (-12, 187), (-11, 194), (-10, 200).

Preparation of $COCl_2 \cdot AsF_5$. A mixture of AsF_5 (12.0 mmol) and $COCl_2$ (30.0 mmol) was stirred at -78 °C for 1 h. The excess of $COCl_2$ was pumped off at -85 °C, leaving behind 3.2g of a white solid (weight calcd for 12.0 mmol of $COCl_2 \cdot AsF_5$ = 3.226 g), melting at -20 ± 2 °C. NMR (SO_2ClF, -60 °C): $COCl_2 \cdot AsF_5$: $\delta(^{13}C)$ 155.9 ppm. $COCl_2$: $\delta(^{13}C)$ 143.7 ppm. Dissociation pressure (temperature [°C], pressure [mm]): (-63, 5), (-60, 9), (-58, 12), (-51, 22), (-44, 49), (-43, 59), (-42, 66), (-40, 85), (-38, 104), (-37, 115), (-35, 143), (-32, 186), (-29, 230), (-28, 260), (-27, 292), (-26, 330), (-25, 375), (-24, 421), (-22, 481).

Preparation of $COCl_2 \cdot SbF_5$. Antimony pentafluoride (4.3 mmol) was dissolved at -78 °C in 5 mL of liquid $COCl_2$. After 5 min the solution became turbid and a precipitate formed. After

1.5 h, the excess of $COCl_2$ was pumped off at -78 °C, leaving behind 4.3 mmol of $COCl_2 \cdot SbF_5$ in the form of a white powder. Dissociation pressure and NMR data could not be measured due to rapid F-Cl exchange resulting in COClF formation.

Computational Methods. The optimized geometries, vibrational spectra and NMR chemical shifts of the O-coordinated carbonyl halide $\cdot MF_5$(M = As, Sb) adducts were calculated using density functional methods. The B3LYP hybrid functional[13] and the Stevens, Basch, Krauss, Jasien and Cundari effective core potentials and the corresponding valence double-zeta basis sets[14] were used. The basis set was augmented with a diffuse s+p shell[15] and a single Cartesian d polarization function on each atom.[16] These calculations, hereafter denoted as B3LYP/SBK+(d), were performed using Gaussian 94 and 98.[17] The calculated Hessian matrices (second derivatives of the energy with respect to Cartesian coordinates) were converted to symmetry-adapted internal coordinates for further analysis with the program systems GAMESS[18] and Bmtrx.[19]

Results and Discussion

Synthesis and Properties of the $COX_2 \cdot MF_5$(X = Cl, F; M = As, Sb) Adducts. Both SbF_5 and AsF_5 form with the an excess of either $COCl_2$, COFCl or COF_2 exclusively O-coordinated 1:1 donor-acceptor complexes (1).

$$MF_5 + COX_2 \xrightarrow[-78^{\circ}C]{COX_2} \underset{(X = F, Cl;\ M = As, Sb)}{COX_2 \cdot MF_5} \qquad (1)$$

The 1:1 compositions were established by the observed material balances and for the COF_2/AsF_5 system by a tensimetric titration (vapor pressure-composition isotherm)[4] at -78 °C which gave evidence only for a 1:1 adduct. The resulting adducts are white solids which are thermally unstable and decompose reversibly to the starting materials, except for the $COCl_2/SbF_5$ system for which rapid irreversible fluorine-chlorine exchange is observed (2).[11]

$$COCl_2 \cdot SbF_5 \longrightarrow COClF + \text{"}SbF_4Cl\text{"} \qquad (2)$$

The oxygen-bridged nature of these adducts was established by vibrational and multinuclear NMR spectroscopy and the results from the theoretical calculations. Only for COClF with at least a threefold excess of SbF_5, does the formation of ionic salts containing the $ClCO^+$ cation become energetically more favorable (3).[1]

$$COClF + 3SbF_5 \longrightarrow ClCO^+Sb_3F_{16}^- \qquad (3)$$

The preferential formation of oxygen-coordinated 1:1 donor-acceptor adducts in these systems is in accord with the previous Raman study of the $COF_2 \cdot MF_5$ (M = As, Sb) systems,[8] a ^{19}F NMR study of the $COClF \cdot SbF_5$ system,[7] and a tensimetric and IR spectroscopic study of the $COCl_2/AlCl_3$ system.[4]

Thermochemical Properties. Based on the vapor pressure data given in the Experimental Section, plots of log P versus T^{-1} for the heterogenous equilibria (4) and (5) give straight lines,

$$COX_2 \cdot AsF_{5\,(s)} \rightleftharpoons COX_{2\,(g)} + AsF_{5\,(g)} \qquad (4)$$

$$COClF \cdot SbF_{5\,(s)} \rightleftharpoons COClF_{(g)} + SbF_{5\,(s)} \qquad (5)$$

which can be described by the following equations:

$COCl_2 \cdot AsF_5$(210-251 °K): log P (mm) = -2486.13/T(°K) + 12.5768

$COClF \cdot AsF_5$(186-231 °K): log P (mm) = -2092.67/T(°K) + 11.649

$COF_2 \cdot AsF_5$(173-218 °K): log P (mm) = -1767.12/T(°K) + 10.5084

$COClF \cdot SbF_5$(230-263 °K): log P (mm) = -3038.9/T(°K) + 13.98

The thermochemical properties, derived from these data by standard procedures,[12] are summarized in Table 1. Literature values were used for the required heats of formation of AsF_5,[20] SbF_5,[21] and the carbonyl halides.[22] Table 1 shows that the stability of the $COX_2 \cdot MF_5$ adducts decreases from SbF_5 to AsF_5, as expected for the decrease in Lewis acidity, and from $COCl_2$ to COF_2, as expected from a decreasing basicity of the oxygen with increasing electron density withdrawal by the more electronegative fluorine ligands. The decrease in the dissociation energy $\Delta H_d°$ from $COClF \cdot AsF_5$

to $COClF \cdot SbF_5$ should not be mistaken as an indication of a weaker adduct. The decrease in $\Delta H_d°$ is caused by the fact that at the investigated dissociation temperatures the SbF_5 decomposition product is a solid and not a gas. Therefore, the value of $\Delta H_d°$ is only one half of that expected for the formation of two moles of gas from one mole of solid. The slopes of the log P versus T^{-1} curves, which are independent of the number of moles of gas in the decomposition products, reflect the expected stability trends, i.e., $COCl_2 \cdot AsF_5$. > $COClF \cdot AsF_5$ > $COF_2 \cdot AsF_5$ and $COClF \cdot SbF_5$ > $COClF \cdot AsF_5$. The same stability trend is also displayed by the extrapolated temperature values at which the adducts would reach a dissociation pressure of one atmosphere (see Table 1). A comparison of the data of Table 1 with the previously reported[4] dissociation pressure of 440 mm at 25 °C for $COCl_2 \cdot AlCl_3$ suggests that the stability of the $COCl_2 \cdot AlCl_3$ adduct is significantly higher than that of $COCl_2 \cdot AsF_5$.

NMR-Spectra. The results of our ^{13}C and ^{19}F NMR study are summarized in Table 2. In agreement with a previous observation,[7] difficulties were encountered in observing well resolved signals for some of the systems at low temperatures due to exchange phenomena. Table 2 shows that on formation of the donor-acceptor adducts both the ^{13}C and ^{19}F signals of the free carbonyl halides are shifted to lower fields, as expected from a deshielding of these nuclei by the electron withdrawing effect of the Lewis acids. These shifts vary from about 5 to 20 ppm and appear to be larger for the stronger Lewis acid SbF_5. The magnitudes and directions of these shifts were confirmed for the $COF_2 \cdot AsF_5$ adduct by our theoretical calculations at the B3LYP/SBK+(d) level of theory using the GIAO method (see Table 2).

The previously reported[3,7] NMR data are for the most part ambiguous. Thus, the report[3] on the $COClF \cdot SbF_5$ adduct in SO_2ClF at -80 °C listed only ^{13}C data with a wide shift range of 150-175 ppm which do not permit a meaningful comparison with the signal of free COClF.

The other previous report[7] dealt only with the ^{19}F spectra of $COF_2 \cdot SbF_5$, $COFCl \cdot SbF_5$ and $COF_2 \cdot AsF_5$ in SO_2ClF solution and also contained some ambiguities. Thus, for $COF_2 \cdot AsF_5$ no

signal for coordinated COF_2 was observed at -100 °C, leading to the incorrect conclusion that even at this low temperature complexation must be incomplete. Furthermore, for a concentrated $COClF/SbF_5$ solution at -80 °C, only signals due to free COF_2 and $COF_2 \cdot SbF_5$ were observed, while for a dilute solution at -95 °C a signal at 59.9 ppm was attributed to $COClF \cdot SbF_5$. However, this shift is almost identical to that of 59.7 ppm found in our study for free COClF and is quite different from that of 73.9 ppm, found by us for the $COClF \cdot SbF_5$ adduct. The only previously well established shift due to complexation appears to be that of 21.7 ppm for the COF_2 - $COF_2 \cdot SbF_5$ pair at -100 °C in SO_2ClF solution, which has been included in Table 2. It supports our conclusion that the stronger Lewis acid SbF_5 deshields the fluorine ligands of the coordinated carbonyl halides more strongly than AsF_5.

Vibrational Spectra and Theoretical Calculations. Vibrational spectra are well suited to distinguish between ionic salts and covalent donor-acceptor adducts.[1,23] As shown by the valence bond structures (6), the C-O and C-X bond orders and, therefore, also their stretching frequencies

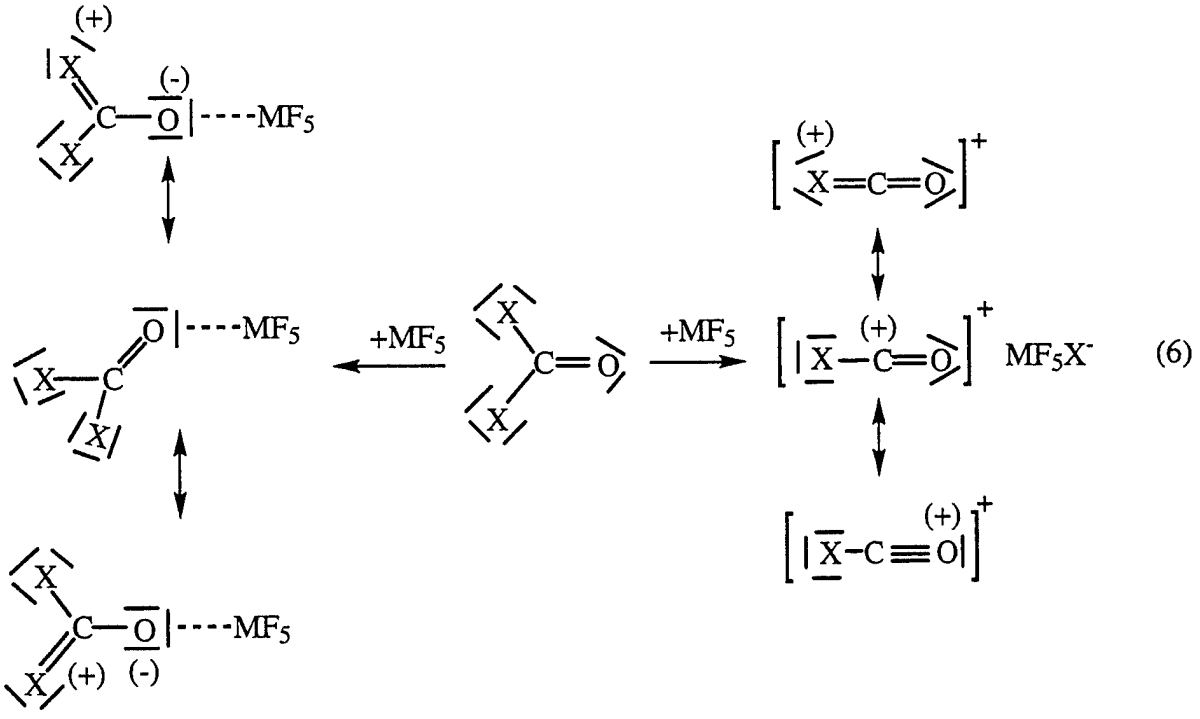

(6)

decrease and the C-X stretching frequencies increase, compared to the free COX_2 molecule. Furthermore, a $COX^+SbF_5X^-$ salt should exhibit only 18 normal modes, while a covalent donor-acceptor adduct should possess 24.

The observed low-temperature Raman spectra of the solid 1:1 complexes of Cl_2CO and ClFCO with AsF_5 and SbF_5 are shown in Figures 1 and 2, and the observed frequencies are summarized in Tables 3 and 4. The large number of observed Raman bands, their frequency shifts relative to the free carbonyl halides,[24] and the excellent fit with the calculated frequencies and intensities (see Tables 3 and 4) leave no doubt that these complexes are O-coordinated donor-acceptor adducts.

Traditionally, the vibrational spectra of this type of covalent donor-acceptor adducts have been analyzed in terms of their separate components in their original point groups, ignoring the bridge modes and the splittings of degenerate modes caused by the symmetry lowering in the adducts. This approach has generally been quite useful and has permitted the analysis of the gross features of the spectra, particularly when the donor-acceptor interactions are relatively weak and the splittings of the degenerate modes are small. However, a rigorous analysis of the finer details of the observed spectra requires a treatment in the correct point group of the adduct, as shown in Table 3. The resulting agreement between the observed and calculated spectra of $COCl_2 \cdot AsF_5$ is very good. The fact that the observed carbonyl stretching frequency is lower and the CCl_2 stretching frequencies are higher than those calculated indicates that in the condensed phase the interactions between the carbonyl halides and the Lewis acids are stronger than those predicted for the free gaseous adducts. Therefore, the calculated optimized geometries, shown in Figure 3, are expected to exhibit somewhat longer M-O and shorter C-O bonds than those expected for the condensed phase. The theoretical results furthermore predict that the modes due to the M-O bridge should occur below 100 cm^{-1} and, hence, justify the traditional approach of neglecting the bridge modes in a vibrational analysis. Finally, it should be noted, that our normal coordinate analyses show that, contrary to the previous assignments[8] and those generally given for closely related C_{4v}

MF_4F species,[25,26] the frequencies of the MF_5 deformation modes decrease in the following order: δscissor MF_4 in plane > δFMF_4 > δumbrella MF_4 > δasym MF_4 in plane.

The observed Raman spectra of $COCl_2 \cdot MF_5$ (M = As, Sb) agree very well with the calculations, except for two extra bands observed for $COCl_2 \cdot SbF_5$ at 442 and 346 cm^{-1}. These bands occur in the Sb-Cl region and are tentatively attributed to some halogen exchange between $COCl_2$ and SbF_5 which is known[11] to occur rapidly at slightly elevated temperatures.

For the $COClF \cdot MF_5$ adducts, two conformers are possible because either the fluorine or the chlorine ligand of COClF could be oriented towards the MF_5 group. The two conformers differ only very little in energy (~0.1 kcal/mol) and their calculated vibrational spectra are almost identical. Therefore, the observed Raman spectra do not allow to distinguish between the two conformers, and the ones with the fluorines pointing toward the MF_5 groups were chosen for our analyses (see Table 4). The MF_5 bands in their COClF adducts agree well with those of the corresponding $COCl_2$ adducts, but the deviations between the observed and calculated bands for the COClF part of the adducts are larger than those for the $COCl_2$ adducts.

For the $COF_2 \cdot MF_5$ adducts, good quality Raman spectra have previously been reported[8] by Chen and Passmore, and their experimental data are compared with our calculations in Table 5. Again, the overall agreement is very satisfactory.

A comparison of the relative changes of the carbonyl halide stretching frequencies within the $COCl_2 \cdot MF_5$, $COFCl \cdot MF_5$ and $COF_2 \cdot MF_5$ series shows that the strength of the adducts increases from COF_2 to $COCl_2$ and from AsF_5 to SbF_5, i.e., with increasing basicity of the donor and increasing acidity of the acceptor. Hence, $COCl_2 \cdot SbF_5$ is the strongest and $COF_2 \cdot AsF_5$ the weakest adduct within this series.

Conclusion

Even with strong Lewis acids, such as AsF_5 or SbF_5, the carbonyl halides, $COCl_2$, COFCl and COF_2, form exclusively O-coordinated donor-acceptor adducts and no ionic salts. The

stability of the adducts increases with increasing basicity of the donor, i.e., from COF_2 to $COCl_2$, and with increasing acidity of the acceptor, i.e., from AsF_5 to SbF_5. This conclusion is strongly supported by thermochemical measurements, vibrational and multinuclear NMR spectroscopy and theoretical calculations.

Acknowledgement. The authors thank Drs. J. Sheehy and G. Olah for their support and one of us (B.H.) the Deutsche Forschungsgemeinschaft for a stipend. The work at USC was supported by the National Science Foundation and that at the Air Force Research Laboratory by the Propulsion Directorate. The computational work was supported in part by a grant of Cray T916 time from the Army Research Laboratory Department of Defense Computing Center and a grant of IBM SP time from the Maui High Performance Computing Center under the sponsorship of the Air Force Research Laboratory.

References

† University of Southern California

‡ Air Force Research Laboratory

§ Current address: Institute of Inorganic Chemistry, University of Cologne, Germany

(1) Christe, K. O.; Hoge, B.; Boatz, J. A.; Prakash, G. K. S.; Olah, G. A.; Sheehy, J. A. *J. Am. Chem. Soc.* in press.

(2) For a recent review see: Ryan, T. A.; Ryan, C.; Seddon, E. A.; Seddon, K. R. *Phosgene and Related Carbonyl Halides*; Topics in Inorganic and General Chemistry, Monograph 24; Clark, R. J H. Ed. Elsevier: Amsterdam, 1996.

(3) Prakash, G. K .S.; Bausch, J. W.; Olah, G. A.; *J. Am. Chem. Soc.* **1991**, *113*, 3203.

(4) Christe, K .O. *Inorg. Chem.* **1967**, *6*, 1706.

(5) Huston, J. L. *J. Inorg. Nucl. Chem.* **1956**, 2, 128.

(6) Dehnicke, K. *Z. Anorg. Allgem. Chem.* **1961**, *312*, 237.

(7) Bacon, J.; Dean, P. A. W.; Gillespie, R. J. *Canad. J. Chem.* **1971**, *49*, 1276.

(8) Chen, G. S. H.; Passmore *J. Chem. Soc. Dalton*, **1979**, 1257.

(9) Christe, K. O.; Wilson, R. D.; Schack, C. *J. Inorg. Synth.* **1986**, *24*, 3

(10) Miller, F. A.; Harney, B. M. *Appl. Spectrosc.* **1969**, *23*, 8.

(11) Hoge, B.; Christe, K. O. *J. Fluor. Chem.*.

(12) (a) Christe, K. O.; Guertin, J. P. *Inorg. Chem.* **1965**, *4*, 905.

(b) Christe, K. O.; Sawodny, W. *Inorg. Chem.* **1967**, *6*, 1783 and **1969**, *8*, 212.

(13) Becke, A. D. *Chem. Phys.* **1993**, *98*, 5648.

(14) (a) Melius, C. F.; Goddard, W. A. *Phys. Rev. A.* **1974**, *10*, 1528.

(b) Kahn, L. R.; Baybutt, P.; Truhlar, D. G. *J. Chem. Phys.* **1976**, *65*, 3826.

(c) Krauss, M.; Stevens, W. J. *Ann. Rev. Phys. Chem.* **1985**, *35*, 357.

(d) Stevens, W. J.; Basch, H.; Krauss, M. *J. Chem. Phys.* **1984**, *81*, 6026.

(e) Stevens, W. J.; Basch, H.; Krauss, M.; Jasien, P. *Can. J. Chem.* **1992**, *70*, 612.

(f) Cundari, T. R.; Stevens, W. J. *J. Chem. Phys.* **1993**, *98*, 5555.

(15) The diffuse s+p function exponents used for Sb, As, Cl, F, O, and C were 0.0259, 0.0287, 0.0483, 0.1076, 0.0845, and 0.0438, respectively.

(16) The d function exponents used for As, Sb and Cl were 0.293, 0.211 and 0.75, respectively. An exponent of 0.8 was used for F, O, and C.

(17) (a) Gaussian 94, Revision E. 2, Frisch, M. J.; Trucks, G. W.; Schlegel, H. B.; Gill, P. M. W.; Johnson, B. G.; Robb, M. A.; Cheeseman, J. R.; Keith, T.; Petersson, G. A.; Montgomery, J. A.; Raghavachari, K.; Al-Laham, M. A.; Zakrzewski, V. G.; Ortiz, J. V.; Foresman, J. B.; Cioslowski, J.; Stefanov, B. B.; Nanayakkara, A.; Challacombe, M.; Peng, C. Y.; Ayala, P. Y.; Chen, W.; Wong, M. W.; Andres, J. L.; Replogle, E. S.; Gomperts, R.; Martin, R. L.; Fox, D. J.; Binkley, J. S.; Defrees, D. J.; Baker, J.; Stewart, J. P.; Head-Gordon, M.; Gonzalez, C.; and Pople, J. A.; Gaussian, Inc. Pittsburgh, PA, **1995**.

(b) Gaussian 98, Revision A. 4, Frisch, M. J.; Trucks,G. W.; Schlegel, H. B.; Scuseria, G. E.; Robb, M.A.; Cheeseman, J. R.; Zakrzewski, V. G.; Montgomery, J. A. Jr.; Stratmann, R. E.; Burant, J. C.; Dapprich, S.; Millam, J. M.; Daniels, A.D.; Kudin, J. N.; Strain, M.c.; Farkas, O.; Tomasi, J.; Barone, V.; Cossie, M.; Cammi, R.; Mennucci, B.; Pomelli, C.; Adamo, C.; Clifford, S.; Ochterski, J.; Petersson, G. A.; Ayala, P. Y.; Cui, Q.; Morokuma, K.; Malick, D. K.; Rabuck, A. D.; Raghavachari, K.; Foresman, J. B.; Cioslowski, J.; Ortiz, J. V.; Stefanov, B. B.; Liu, G.; Liaschenko, A.; Piskorz, P.; Komaromi, I.; Gomperts, R.; Martin, R. L.; Fox, D. J.; Keith, T.; Al-Laham, M. A.; Peng, C.Y.; Nanayakkara, A.; Gonzalez, C.; Challacombe, M.; Gill, P. M. W.; Johnson, B.; Chen, W.; Wong, M. W.; Andres, J. L.; Gonzalez, C.; Head-Gordon, M.; Replogle, E. S.; and Pople J. A. Gaussian, Inc., Pittsburgh PA, **1998**.

(18) Schmidt, M. W.; Baldridge, K. K.; Boatz, J. A.; Elbert, S. T.; Gordon, M. S.; Jensen, J. H.; Koseki, S.; Matsunaga, N.; Nguyen, K. A.; Su, S. J.; Windus, T. L.; Dupuis, M.; Montgomery, J. A. *J. Comput. Chem.* **1993**, *14*, 1347.

(19) Bmtrx version 2.0; Komornicki, A.; Polyatomics Research Institute: Palo Alto, CA **1996**.

(20) Barin, I.; Knacke, O.; Kubaschewski, O. "Thermochemical Properties of Inorganic Substances," Supplement, **1977**, Springer Verlag.

(21) Bougon, R.; Bui Huy, T.; Burgess, J.; Christe, K. O.; Peacock, R. D. *J. Fluor. Chem.* **1982**, *19*, 263.

(22) "JANAF Interim Thermochemical Tables," The Dow Chemical Co., Midland, Mich., **1965**, and subsequent revisions.

(23) Lindquist, I. "Inorganic Adduct Molecules of Oxo-Compounds," Anorganische und Allgemeine Chemie in Einzeldarstellungen, Band IV, Becke-Goehring, M. Ed.; Academic Press Inc., New York, **1963**.

(24) (a) Shimanouchi, T. *J. Phys. Chem. Ref. Data* **1977**, *6*, 993, and references cited therein. (b) Shimanouchi, T. "Tables of Molecular Vibrational Frequencies, Consolidated Volume 1," NSRDS-NBS39, Nat. Stand. Ref. Data Ser.,Nat. Bur. Stand. (U.S.), **1972**, and references cited therein.

(25) Siebert, H. "Anwendungen der Schwingungsspektroskopie in der Anorganischen Chemie," Anorganische und Allgemeine Chemie in Einzeldarstellungen, Band VII, Becke-Goehring, M. Ed.; Springer Verlag, Berlin Heidelberg, New York, **1966**.

(26) Nakamoto, K. "Infrared and Raman Spectra of Inorganic and Coordination Compounds, Part A," Fifth Edition, John Wiley & Sons, New York, **1997**.

Table 1. Thermochemical Data for the Dissociation of the $X_2CO{\cdot}MF_5$ Donor-Acceptor Adducts and Their Heats of Formation.

	$\Delta H_d°$ [a] kcal/mol	T(1 atm) [b] °C	P_{298} [c] atm	$\Delta F°_{298}$ [d] kcal/mol	$\Delta S°_{298}$ [e] cal/deg mol	$\Delta H°_{f\,298}(X_2CO{\cdot}AsF_5)$ [f] kcal/mol
$Cl_2CO{\cdot}AsF_5$	22.75	-16.8	22.78	-2.882	85.98	-370.81
$ClFCO{\cdot}AsF_5$	19.15	-34.5	56.15	-3.951	77.49	-416.61
$F_2CO{\cdot}AsF_5$	16.17	-41.5	50.19	-3.818	67.05	-464.33
$ClFCO{\cdot}SbF_5$	13.91	0.6	8.07	-0.826	49.41	-433.15

[a]Enthalpies of dissociation, calculated from the slope of the log P vs T^{-1} curves. [b]Extrapolated temperatures at which the dissociation pressures of the solid adducts would reach a dissociation pressure of 760 mm. [c]Extrapolated dissociation pressures at 298°K. [d]Values for the free energy change at 298 °K. [e]Values for the entropy changes at 298 °K. [f]Standard heats of formation of the solid adducts using the dissociation enthalpies of this work and the following literature values for the heats of formation: $\Delta H_f°_{298}(COCl_{2(g)}) = -52{,}600$; $\Delta H_f°_{298}(COFCl_{(g)}) = -102.00$; $\Delta H_f°_{298}(COF_{2(g)}) = -152.700$; $\Delta H_f°_{298}(AsF_{5\,(g)}) = -295.461$; $\Delta H_f°_{298}(SbF_{5\,(l)}) = -317.248$ kcal/mol.

Table 3. Calculated (B3LYP/SBK+(d) Vibrational Frequencies and Observed Raman Spectra of the $COCl_2 \cdot MF_5$ (M=As, Sb) Adducts and their Analyses Based on the Point Groups of the Adducts and the Individual Donor and Acceptor Molecules

assignments, approx mode descript			freq, cm^{-1}, intensities [a]			
			$COCl_2 \cdot AsF_5$		$COCl_2 \cdot SbF_5$ [c]	
MF_5 C_{4v}	$COCl_2$ C_{2v}	$COCl_2 \cdot MF_5$ C_s	obsd Ra	calcd (IR)[Ra]	obsd Ra	calcd (IR)[Ra]
	$\nu_1(A_1)$1827	$\nu(A')$vc=o	1610[33]	1768(671)[43]	1587[14]	1718(740)[29]
	$\nu_4(B_1)$849	$\nu_2(A')$vas CCl_2	978[11]	896(460)[9.7]	989[3.4]	930(430)[6.1]
$\nu_7(E)$		$\nu_3(A')$vas MF_4	770[4]	734(127)[.35]	708[2]	667(90)[2.2]
		$\nu_{16}(A'')$vas MF_4	733[1]	736(152)[.09]	—	667(114)[.13]
$\nu_1(A_1)$		$\nu_4(A')\nu$ MF'	757[44]	742(153)[8.3]	683[22]	665(114)[5.5]
$\nu_2(A_1)$		$\nu_5(A')$vs MF_4in phase	698[100]	663(1. 7)[30]	654[100]	617(5.7)[34]
	$\nu_2(A_1)$567	$\nu_6(A')$ vs CCl_2	660[52]	597(8.4)[16.4]	676[66]	623(.27)[3.9]
$\nu_4(B_1)$		$\nu_{17}(A'')$ vs MF_4 out of phase	615[15]	597(.21)[2.8]	608[16]	577(.34)[2.3]
	$\nu_6(B_2)$580	$\nu_{18}(A'')$ δ MOCCl out of plane	592[2]	582(3.3)[.02]	600sh	585(3.3)[.08]
	$\nu_5(B_1)$440	$\nu_7(A')$ δ MOCCl in plane	538[22]	471(.25)[4.6]	528[9]	484(2.7)[4.1]
$\nu_3(A_1)$		$\nu_8(A')$ δ sciss MF_4	402[19]	403(.03)[1.6]	303[.21]	307(.12)[1.5]
$\nu_8(E)$		$\nu_{19}(A'')$ δ FMF_4 out of plane	391[4]	380(47)[.26]	286[8]	287(53)[.34]
		$\nu_9(A')$ δ FMF_4 in plane	380[11]	379(42)[.33]	279[4]	283(46)[.18]
	$\nu_3(A_1)$285	$\nu_{10}(A')$ δ sciss CCl_2	360[33]	308(46)[4.2]	394[37]	322(2.7)[5.1]
$\nu_6(B_2)$		$\nu_{11}(A')$ δ umbrella MF_4	328[15]	331(83)[2.4]	260[2]	262(141)[.17]
$\nu_9(E)$		$\nu_{12}(A')$ δ as MF_4 in plane	304[29]	276(.88)[1.7]	236[16]	221(.90)[1.3]
		$\nu_{20}(A'')$ δ as MF_4 in plane	238[11]	278(.63)[.84]	—	233(.48)[.42]
		$\nu_{21}(A'')$ δ wag $COCl_2$	181[14]	165(.20)[.61]	190[21]	165(.20)[.85]
		$\nu_{13}(A')$ δ rock $COCl_2$	140[13]	125(1.2)[.55]	146[22]	134(8.4)[.91]
$\nu_5(B_1)$		$\nu_{22}(A'')$ δ pucker MF_4	—	115(0)[0]	—	119(0)[.01]
		$\nu_{14}(A')$ νM-O	—	74(15)[.04]	—	104(13)[.15]
		$\nu_{15}(A')$ δM-O-C	—	49(1.9)[.36]	—	60(.04)[,18]
		$\nu_{23}(A'')$ τ c-o	—	38(.15)[1.2]	—	45(.06)[.88]
		$\nu_{24}(A'')$ τ M-O	—	16(.09)[1.2]	—	24(1.0)[1.38]

[a]Calculated infrared and Raman intensities in km/mol and $Å^4$ /amu, respectively. [b]Data from ref. 24.
[c]In the Raman spectrum of solid $COCl_2 \cdot SbF_5$ two additional bands were observed at 442[8] and 346[15] cm^{-1} which were of variable intensity and probably do not belong to the adduct (see text).

Table 4. Calculated (B3LYP/SBK + (d)) Vibrational Frequencies and Observed Raman Spectra of the COClF·MF_5 (M = As, Sb) Adducts and their Analyses Based on the Point Groups of the Adducts and the Individual Donor and Acceptor Molecules

assignments, approx mode descript			freq, cm^{-1}, intensities			
MF_5	COClF	COClF·MF_5	COClF·AsF_5		COClF·SbF_5	
			obsd	calcd[c]	obsd	calcd[c]
C_{4v}	Cs obsd[a]	Cs	Ra	(IR)[Ra]	Ra	(IR)[Ra]
	ν_1 (A') 1868	ν_1 (A') νc = o	1701[40]	1826(695)[38]	1669[8]	1789(751)[25]
	ν_2 (A') 1095	ν_2 (A') νcF	1220[1]	1167(416)[4]]	1257(vs)[b]	1208(412)[2.0]
ν_7 (E)		ν_3 (A') νas MF_4 ν_{16} (A") νas MF_4	780[5] 732[5]	735(147)[.17] 736(160)[.06]	712[2]	667(112)[2.0] 670(126)[.22]
ν_1 (A_1)		ν_4 (A') ν MF'	742[52]	743(173)[5.8]	689[42]	668(106)[4.0]
ν_2 (A_1)		ν_5 (A') νs MF_4 in phase	695[100]	663(2.2)[31]	651[100]	621(2.3)[28]
	ν_3 (A') 776	ν_6 (A') ν CCl	835[35]	781(47)[15]	842[21]	795(50)[13]
ν_4 (B_1)		ν_{17} (A") νs MF_4 out of phase	616[16]	597(.13)[3.1]	603[15]	578(.36)[2.6]
	ν_6 (A") 667	ν_{18} (A") δ MO CCl out of plane	580[4]	659(8.5)[.32]	590[2]	660(2.4)[.20]
	ν_4 (A') 501	ν_7 (A') δ MO CCl in plane	453[16]	520(2.1)[5.2]	470[15]	536(6.8)[3.4]
ν_3 (A_1)		ν_8 (A') δ sciss MF_4	401[13]	404(.01)[1.6]	301[18]	308(.08)[1.6]
ν_8 (E)		ν_{19} (A") δ FMF_4 out of plane ν_9 (A') δ FMF_4 in plane	390[4] 382[2]	380(48)[.25] 379(43)[.26]	275[3]	287(53)[.30] 285(49)[.29]
	ν_5 (A') 415	ν_{10} (A') δ sciss ClCF	340[9]	420(.29)[2.3]	337[3]	429(1.9)[2.4]
ν_6 (B_2)		ν_{11} (A') δ umbrella MF_4	325[3]	327(125)[1.9]	265[2]	264(134)[.27]
ν_9 (E)		ν_{12}(A') δ as MF_4 in plane ν_{20} (A") δ as MF_4 in plane	306[10] 233[5]	276(.83)[1.0] 278(.69)[.86]	240[8]	223(.98)[.79] 232(.77)[.41]
		ν_{21}(A") δ wag COClF	197[4]	164(.12)[.45]	198[20]	165(.13)[.73]
		ν_{13}(A') δ rock COClF	148[17]	137(1.2)[.13]		146(5.5)[.60]
ν_5 (B_1)		ν_{22}(A") δ pucker MF_4		114(0)[0]		115(0)[0]
		ν_{14} (A') ν M-O		76(15)[.21]		109(14)[.20]
		ν_{15}(A') δ M-O-C		53(1.6)[.31]		62(.05)[.27]
		ν_{23}(A") τ c=o		36(.13)[1.1]		41(.06)[.64]
		ν_{24}(A") τ M-O		28(.02)[.51]		32(.01)[.81]

[a]Data from ref 2.4. [b]Frequency and intensity from the infrared spectrum. [c]The listed calculated frequencies are for the isomers in which the fluorine atom of the COClF unit is pointed toward MF_5.

Table 5. Calculated (B3LYP/SBK+(d)) Vibrational Frequencies and Literature [a]Raman Spectra of the $COF_2 \cdot MF_5$ (M = As, Sb) Adducts and their Analyses .

___assignments, approx mode descript _____			____freq, cm^{-1}, intensities_____			
MF_5	COF_2	$COF_2 \cdot MF_5$	_____$COF_2 \cdot AsF_5$ _____		_____ $COF_2 \cdot SbF_5$ _____	
C_{4v}	C_{2v} obsd[b]	Cs	obsd Ra	calcd (IR)[Ra]	obsd Ra	calcd (IR)[Ra]
	$\nu_1(A_1)$1928	$\nu_1(A')$νc=o	1788[12]	1896(704)[22]	1770[9]	1866(753)[13]
	$\nu_4(B_1)$1249	$\nu_2(A')$νas CF_2	1402[5]	1314(407)[4.2]	1436[4]	1360(398)[3.3]
$\nu_7(E)$		$\nu_3(A')$νas MF_4	776[7]	736(146)[.48]	716[19]	669(108)[2.0]
		$\nu_{16}(A'')$νas MF_4	~735[7]	736(117)[.11]	701[29]	669(108)[.12]
$\nu_1(A_1)$		$\nu_4(A')$ν MF'	765[18]	746(142)[6.1]	673[82]	671(98)[4.1]
$\nu_2(A_1)$		$\nu_5(A')$νs MF_4in phase	701[100]	664(2.8)[26]	658[100]	622(2.2)[23]
	$\nu_2(A_1)$965	$\nu_6(A')$ νs CF_2	1037[20]	993(3.7)[9.8]	1050[28]	1013(26)[10]
$\nu_4(B_1)$		$\nu_{17}(A'')$ νs MF_4 out of phase	615[16]	597(.28)[3.1]	600[23]	578(.64)[2.6]
	$\nu_6(B_2)$774	$\nu_{18}(A'')$ δ $MOCF_2$ out of plane	792[3]	756(74)[.56]	774[6]	757(43)[.52]
	$\nu_5(B_1)$626	$\nu_7(A')$ δ $MOCF_2$ in plane	673[4]	623(13)[1.5]	coincid.[d]	634(16)[3.3]
$\nu_3(A_1)$		$\nu_8(A')$ δ umbrella MF_4	406[13]	405(.02)[1.7]	303[28]	309(.09)[1.6]
$\nu_8(E)$		$\nu_{19}(A'')$ δ FMF_4 out of plane	351[4][e]	381(48)[.19]	285[5]	288(52)[.19]
		$\nu_9(A')$ δ FMF_4 in plane		380(45)[.20]		285(50)[.21]
	$\nu_3(A_1)$584	$\nu_{10}(A')$ δ sciss CF_2	606[4]	575(3.9)[1.0]	606 sh	581(3.0)[1.0]
$\nu_6(B_2)$		$\nu_{11}(A')$ δ sciss MF_4	328[7]	332(96)[.68]	265[14]	268(101)[.19]
$\nu_9(E)$		$\nu_{12}(A')$ δ as MF_4 in plane	308[9]	276(.95)[1.1]	226[14]	222(2.8)[.98]
		$\nu_{20}(A'')$ δ as MF_4 in plane	238[4]	277(.84)[1.0]	242[14]	232(1.3)[.69]
		$\nu_{21}(A'')$ δ wag COF_2	—	165(.05)[. 19]	194[19]	167(.04)[.37]
		$\nu_{13}(A')$ δ rock COF_2	—	142 (5.4)[.07]	—	163(20)[.17]
$\nu_5(B_1)$		$\nu_{22}(A'')$ δ pucker MF_4	—	108(0)[0]	—	112(0)[0]
		$\nu_{14}(A')$ νM-O	—	87(14)[.15]	—	115(7.9)[.09]
		$\nu_{15}(A')$ δM-O-C	—	55(.82)[.01]	—	65(0)[.03]
		$\nu_{23}(A'')$ τ c=o	—	42(.01)[.47]	—	47(0)[.40]
		$\nu_{24}(A'')$ τ M-o	—	24(.20)[.27]	—	34(.20)[.25]

[a]The observed frequencies were taken from ref 8. [b]Data from ref 24. [c]Weak bands shown in the Figures, but not listed in the tables of ref 8. [d]Coincidence with either 658[100] or 673[82]. [e]Figure 3 of ref 8 shows weak bands in the 380 cm^{-1} region, which might also belong to ν_{19} and ν_9 of the adduct.

DIAGRAM CAPTIONS

Figure 1. Raman spectra of solid $COCl_2 \cdot AsF_5$ (upper trace) and $COCl_2 \cdot SbF_5$ (lower trace) recorded at -130 °C.

Figure 2. Raman spectra of solid $COClF \cdot AsF_5$ (upper trace) and $COClF \cdot SbF_5$ (lower trace) recorded at -130 °C.

Figure 3. Geometries optimized at the B3LYP/SBK +(d) level for $COCl_2 \cdot MF_5$, $COClF \cdot MF_5$ and $COF_2 \cdot MF_5$ where M = As(Sb).

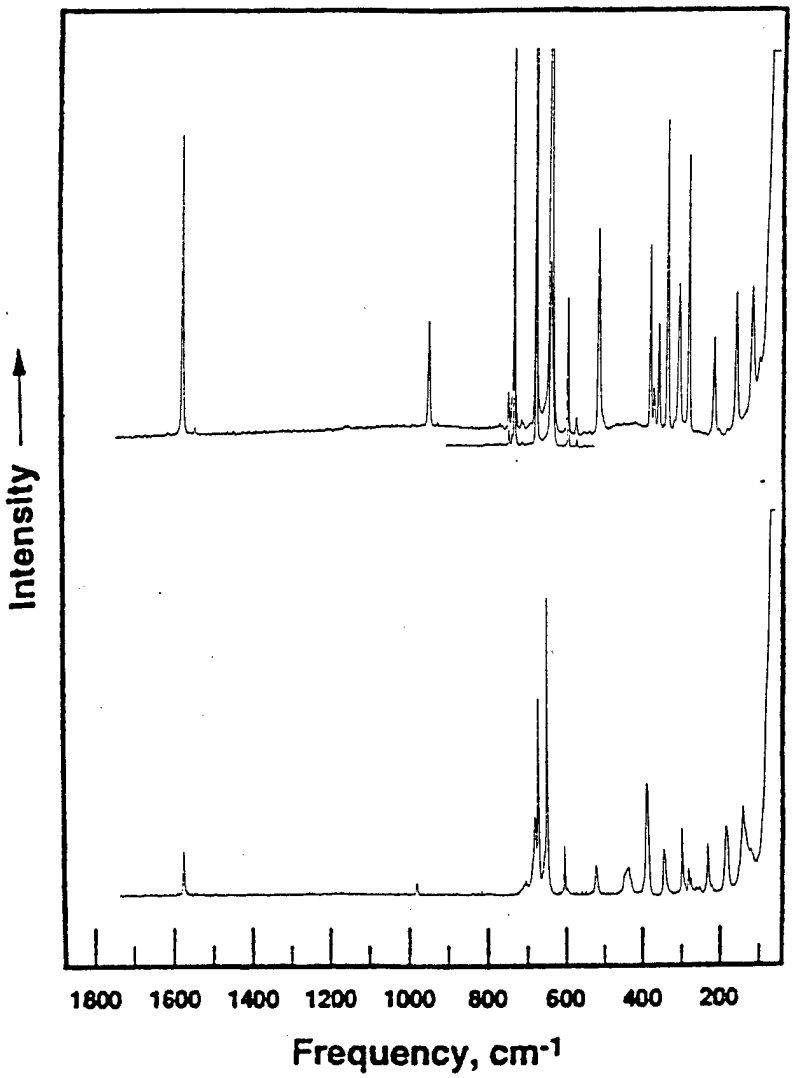
Intensity
1800
1600
1400
1200
1000
800
600
400
200
Frequency, cm-1

FIGURE 1

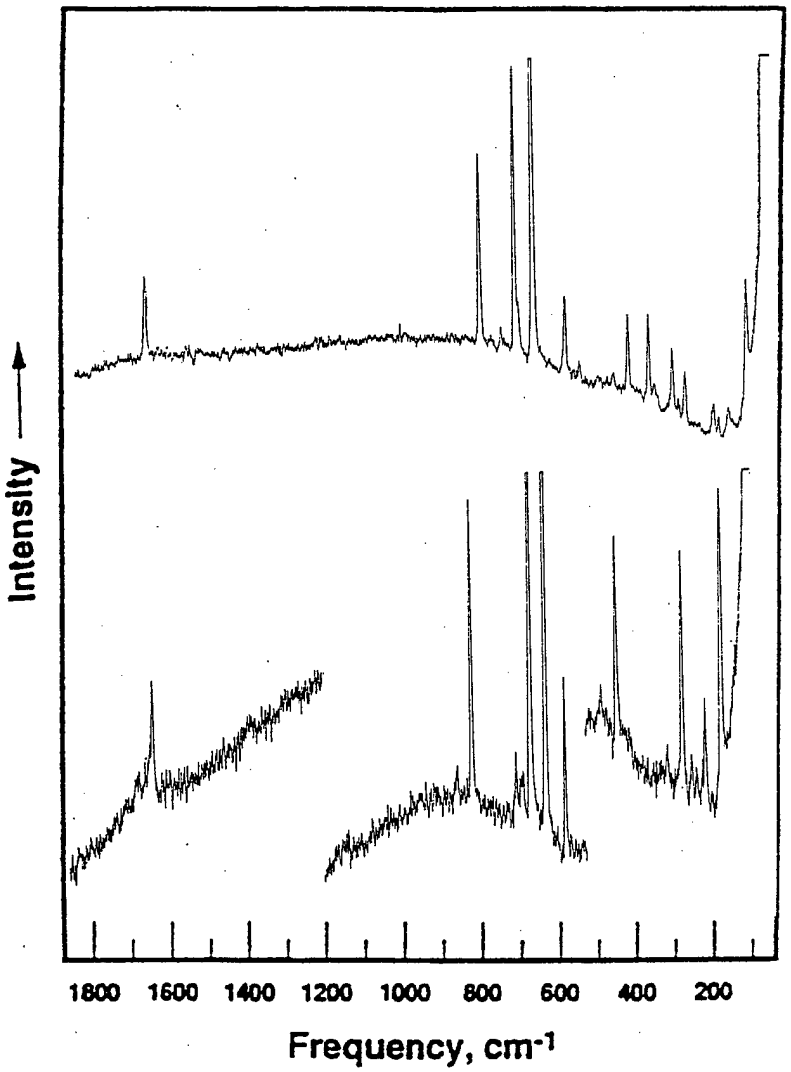
Intensity
1800
1600
1400
1200
1000
800
600
400
200
Frequency, cm-1

FIGURE 2

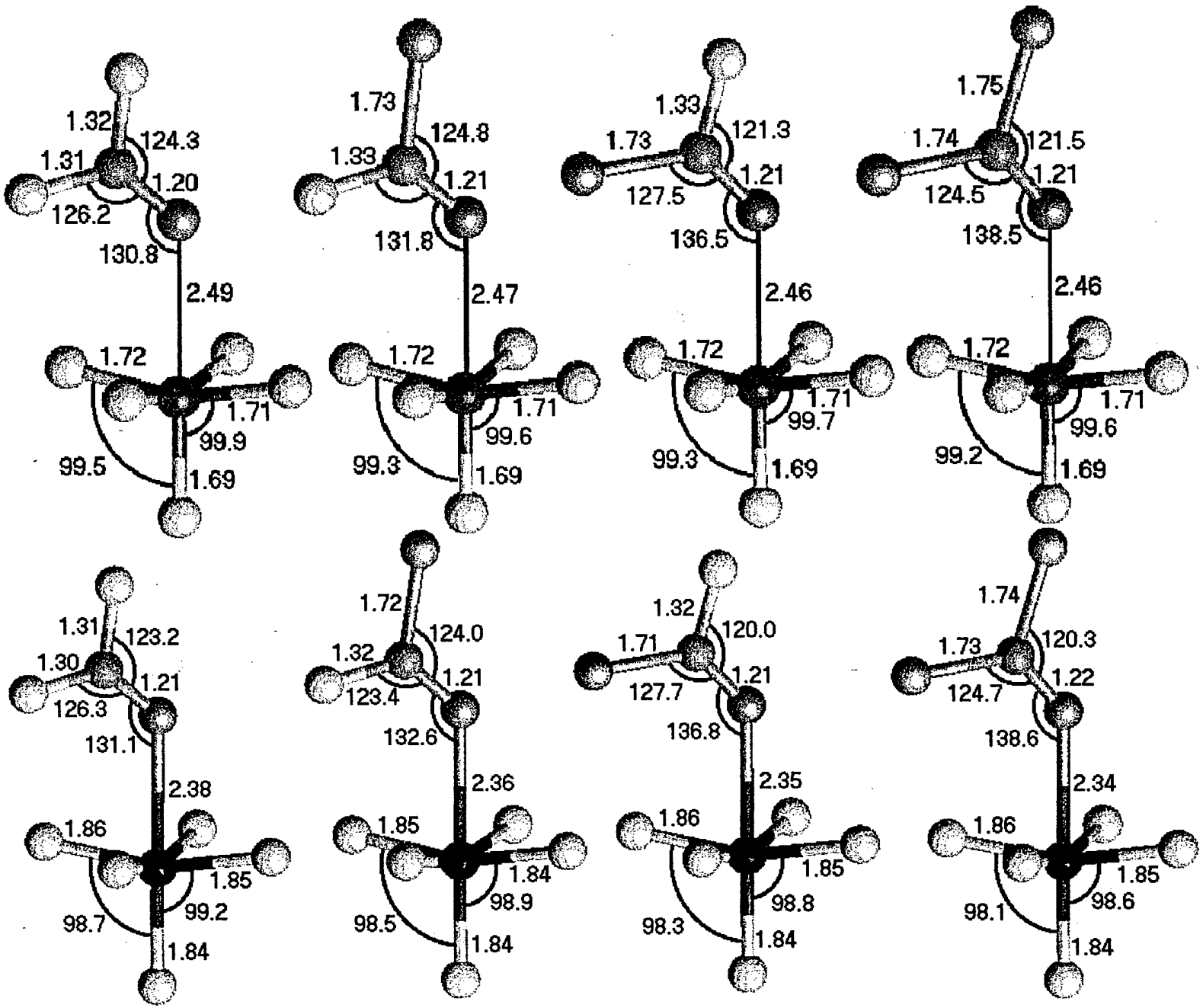
1.32
124.3
1.31
1.20
126.2
130.8
2.49
1.72
1.71
99.9
99.5
1.69
1.73
124.8
1.33
1.21
131.8
2.47
1.72
1.71
99.6
99.3
1.69
1.33
121.3
1.73
1.21
127.5
136.5
2.46
1.72
1.71
99.7
99.3
1.69
1.75
1.74
121.5
1.21
124.5
138.5
2.46
1.72
1.71
99.6
99.2
1.69
1.31
123.2
1.30
1.21
126.3
131.1
2.38
1.86
1.85
99.2
98.7
1.84
1.72
124.0
1.32
1.21
123.4
132.6
2.36
1.85
1.84
98.9
98.5
1.84
1.32
120.0
1.71
1.21
127.7
136.8
2.35
1.86
1.85
98.8
98.3
1.84
1.74
120.3
1.73
1.22
124.7
138.6
2.34
1.86
1.85
98.6
98.1
1.84